

## Modeling of Copper(II) Complexes with the SIBFA Polarizable Molecular Mechanics Procedure. Application to a New Class of HIV-1 Protease Inhibitors

Marie Ledecq,<sup>\*,†</sup> Florence Lebon,<sup>§,†</sup> François Durant,<sup>†</sup> Claude Giessner-Prettre,<sup>‡</sup> Antonio Marquez,<sup>||</sup> and Nohad Gresh<sup>⊥</sup>

Facultés Universitaires Notre-Dame de la Paix, Laboratoire de Chimie Moléculaire Structurale, 61 rue de Bruxelles, 5000 Namur, Belgium, Laboratoire de Chimie Théorique, UMR7615, Université Pierre & Marie Curie, 4, place Jussieu, 75252 Paris, France, Departamento de Química Física, Facultad de Química, Universidad de Sevilla, E-41012 Sevilla, Spain, and Laboratoire de Pharmacochimie Moléculaire et Structurale, FRE 2463 CNRS, U266 INSERM, Université René Descartes, 4, avenue de l'Observatoire, 75006 Paris, France

Received: May 26, 2003; In Final Form: August 1, 2003

We have previously developed a new family of organometallic complexes targeting the HIV-1 protease, an enzyme that is essential for viral maturation. Among these, two  $\text{Cu}^{2+}$  complexes **C1** and **C2** were synthesized from flexible ligands **L1**, *N1*-(4-methyl-2-pyridyl)-2,3,6-trimethoxybenzamide and **L2**, *N2*-(2-methoxybenzyl)-2-quinolinecarboxamide, respectively. These ligands, designed to fit the protease active site, were shown to form 2:1 complexes with  $\text{Cu}^{2+}$ . To compare the relative stability of **C1** and **C2** and to study the energetic and structural aspects of such large  $\text{Cu}^{2+}$  complexes, we have extended the polarizable molecular mechanics procedure SIBFA to treat this cation. This was done by carrying out parallel ab initio (HF, MP2) as well as DFT computations. A first validation step was done on monoligated complexes, in which the SIBFA energy components were shown to correctly match their ab initio counterparts from an energy-decomposition procedure. Subsequent tests on polyligated  $\text{Cu}^{2+}$  complexes with neutral and anionic ligands showed the procedure to reproduce the results from MP2 and DFT computations with good accuracy (relative error <3%). We have next extended the calculations to compare the **C1** and **C2** complexes. Energy balances including continuum solvation effects indicate a greater stability of the **C1** complex, in agreement with experimental results. The effects of the methoxyphenyl substituents on the **C1** complex stability were further investigated and compared to their concomitant influences on the ab initio-computed molecular electrostatic potential.

### Introduction

Enzyme inhibitors used as therapeutic agents are usually organic molecules that interact with the target protein mainly through hydrogen bonding and van der Waals contacts. In the recent years, however, an increasing interest has been given to organometallic compounds that hold the attractive promise of forming stronger interactions with the target protein by combining the coordination ability of metals (covalent and ionic bonding) with the stereoelectronic properties of the organic ligand (hydrogen bonding and van der Waals contacts).<sup>1,2</sup> As complexes with transition metals have successfully been used to inhibit proteins,<sup>3,4</sup> we used de novo drug design to investigate the potency of organometallic compounds to act as inhibitors of the HIV-1 protease (PR).<sup>5–7</sup> The HIV-1 PR activity is essential for viral maturation and this protein is thus considered as a major target in the treatment of AIDS.<sup>8</sup> The catalytic mechanism of this aspartic protease typically involves a water molecule. We based our design on the hypothesis that a metal ion would ideally bind this HIV-1 PR structural catalytic water molecule. On the basis of the typical octahedral geometry of

the  $\text{Cu}^{2+}$  complexes, we designed  $\text{Cu}^{2+}$  chelating ligands with optimal geometry to interact with HIV-1 PR binding pockets.<sup>5,6</sup> Among these, *N1*-(4-methyl-2-pyridyl)-2,3,6-trimethoxybenzamide and *N2*-(2-methoxybenzyl)-2-quinolinecarboxamide were synthesized and complexed to  $\text{Cu}^{2+}$ . The structure of these complexes (respectively referred as **C1** and **C2**) was determined by X-ray crystallography and confirms that these compounds adopt an adequate geometry to interact with HIV-1 PR<sup>6</sup> (Figure 1). Kinetic and EPR experiments were performed and showed that **C1** acts as a competitive inhibitor of HIV-1 PR with a  $K_i$  in the low micromolar range. In contrast, we showed that **C2** is not stable enough in the assay buffer (NaOAc 0.1 M, pH = 5.5) to act as an inhibitor of HIV-1 PR but releases  $\text{Cu}^{2+}$  in the medium.<sup>7</sup> To rationalize the design of organometallic inhibitors with increased stability, we developed a procedure to predict this key property.

Force fields which can accurately reproduce the structural features of  $\text{Cu}^{2+}$  complexes have been recently put forth,<sup>9</sup> some containing an additional term conceived to reproduce the ligand field effect on d electron orbitals.<sup>10,11</sup> In these approaches, one uses a classical formulation of the potential energy with an additional set of potential functions for the metal–ligand interactions. For the present purposes, however, if we are to address the issue of differential stabilities of competing candidate ligands, it is clear that, in addition to a reliable structural description, an accurate value of the interaction energies is also necessary.

\* To whom correspondence should be addressed. Phone: +32 81 724569. Fax: +32 81 724530. E-mail: marie.ledecq@fundp.ac.be.

<sup>†</sup> Facultés Universitaires Notre-Dame de la Paix.

<sup>‡</sup> Université Pierre & Marie Curie.

<sup>§</sup> Current address: UCB S. A. Chemin du Foriest, B-1420 Braine-l'Alleud, Belgium.

<sup>||</sup> Universidad de Sevilla.

<sup>⊥</sup> Université René Descartes.

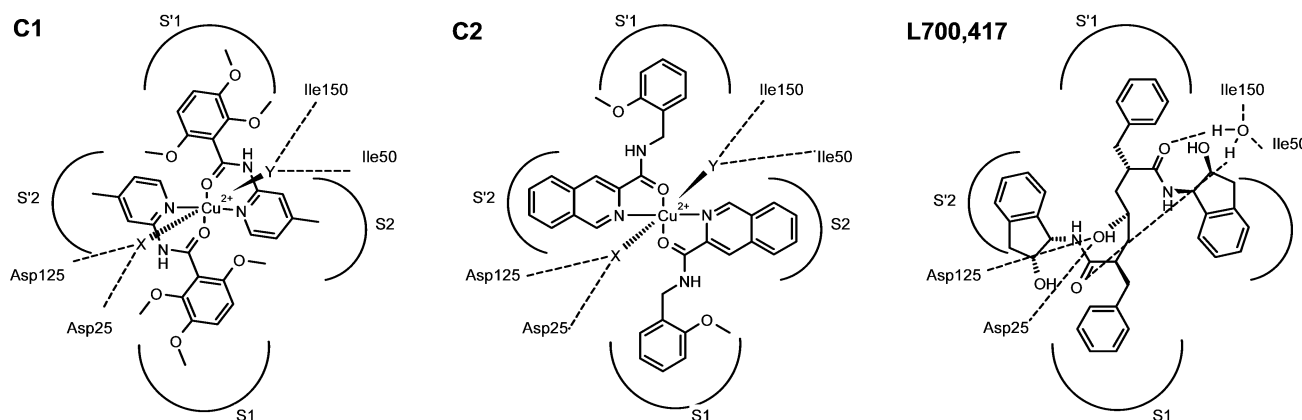


**Figure 1.** Structure of complexes **C1** and **C2**. These compounds were designed to interact with the HIV-1 PR subsites (S1, S2, S'1 and S'2). From a preliminary molecular modeling study,<sup>5</sup> the interaction of the Cu<sup>2+</sup> complexes with Asp25 and Asp125 side chains in the HIV-1 PR was assumed to occur through the catalytic water molecule while the interaction of Cu<sup>2+</sup> complexes with Ile50 and Ile150 main chain was assumed to occur through ligand Y, a key structural water molecule in PR. In a classical peptidomimetic inhibitor such as L700,417,<sup>54</sup> the catalytic water molecule is displaced by a hydroxyl substituent of the inhibitor while the structural water molecule is hydrogen bonded with both the inhibitor and the PR.

Quantum-chemical (QC) *ab initio* and DFT calculations constitute the most reliable approach to compute the complexation energies of Cu<sup>2+</sup> with small-sized ligands. With dedicated computational facilities, these QC approaches can be extended to larger Cu<sup>2+</sup> complexes, such as those of **C1** and **C2**. However, the docking of such complexes in the active site of the HIV-1 protease involves their interactions with the relevant amino acids of the site, which could encompass more than 100 atoms. Although the use of QM/MM procedures can be considered, the substantial increase in CPU time could preclude a thorough investigation of the potential energy surface and the investigation of numerous, possibly more efficient derivatives. In addition, the nonpolarizable nature of the MM part could also limit the accuracy of the energy balances, because the electrostatic field exerted by the dipositive charge of Cu<sup>2+</sup> could exert itself beyond the active site. A possible alternative to QM/MM consists of polarizable molecular mechanics, in which the whole molecular complex is treated with the same energy function throughout. As a preliminary step toward docking studies of Cu<sup>2+</sup> complexes, we have sought to extend the polarizable molecular mechanics procedure SIBFA (sum of interactions between fragments *ab initio* computed)<sup>12–14</sup> to handle the Cu<sup>2+</sup> cation and use it to analyze the factors responsible for the relative stabilities of complexes **C1** and **C2**. Indeed, attainment of a minimal stabilization energy is an essential feature to prevent release of Cu<sup>2+</sup> and complex dissociation in water before the protein target is reached. The SIBFA methodology has previously been formulated and calibrated on the basis of *ab initio* SCF supermolecule computations together with intermolecular interaction energy decomposition.<sup>15</sup> The SIBFA computations were already applied successfully to study the energetics of Zn<sup>2+</sup>,<sup>16–21</sup> Cu<sup>+</sup>,<sup>22</sup> Mg<sup>2+</sup>, Ca<sup>2+</sup>, and Cd<sup>2+</sup><sup>23</sup> binding to biologically relevant ligands and validated by systematic comparisons of the results with *ab initio* SCF calculations. It was also used to study drug metallo-enzyme complexes.<sup>24,25</sup>

The organization of this paper is as follows. We first analyze by an energy-decomposition procedure the Hartree–Fock (HF) and MP2 interaction energies of monoligated complexes of Cu<sup>2+</sup> with its most frequently encountered O- and N-containing ligands and evaluate in parallel the accuracy of the SIBFA procedure. This is followed by the investigation of several representative, neutral and ionic, polyligated complexes of Cu<sup>2+</sup> and of two binuclear Cu<sup>2+</sup> complexes. The interaction energies of these polyligated complexes are computed at Hartree–Fock,

MP2, and DFT/B3LYP levels using SIBFA energy-minimized structures. These important tests should allow the evaluation of the accuracy of the procedure upon substantial increases of the binding energies and onset of nonadditivity. They are then extended to reduced models of **C1** and **C2**, each of which is considered in two competing arrangements. After these validation steps, we use SIBFA to investigate the structural and energetical features of the Cu<sup>2+</sup> complexes of **C1** and **C2**. This is extended to several derivatives of **C1**, which differ by the number and location of methoxy substituents, to unravel their individual effects on the complex stability. We perform energy balances for their complexation in water and evaluate in parallel how these substituents modulate the molecular electrostatic potential at the cation-binding position.

### Computational Procedure

In the SIBFA procedure,<sup>14,16</sup> the intermolecular interaction energy  $\Delta E_{\text{int}}$  is computed as the sum of five separate contributions, namely (eq 1)

$$\Delta E_{\text{int}} = E_{\text{MTP}} + E_{\text{rep}} + E_{\text{pol}} + E_{\text{ct}} + E_{\text{disp}} \quad (1)$$

$E_{\text{MTP}}$  is the electrostatic (multipolar) component, computed as a sum of multipole–multipole interaction terms. The multipoles (up to quadrupoles) are distributed on the atoms and bonds of the individual molecules or molecular fragments making up a larger molecule. They are derived from the *ab initio* SCF molecular wave function using the procedure developed by Vigné-Maeder and Claverie.<sup>26</sup>

$E_{\text{rep}}$  is the short-range repulsion energy. To account for its anisotropic character, it is computed as a sum of bond–bond, bond–lone pair, and lone pair–lone pair interactions. The formulation of  $E_{\text{rep}}$  takes into account the explicit hybridization nature of the bonds, in addition to that of the lone pairs. The expression of  $E_{\text{rep}}$  was detailed in refs 16 and 27 for the general case and for ligand–cation interactions, respectively.

$E_{\text{pol}}$  is the polarization energy component, calculated with distributed anisotropic polarizabilities on the individual molecular fragments. The polarizabilities are distributed on the centroids of the localized orbitals (heteroatom lone pairs and bond barycenters) using the procedure of Garmer and Stevens.<sup>28</sup> A Gaussian screening of the polarizing field is used (see ref 27 for details). The *ab initio* computations were done with the GAMESS software.<sup>29</sup>

$E_{\text{ct}}$  is the charge-transfer contribution. The numerator of  $E_{\text{ct}}$  is a function of the overlap between the lone pair hybrids of the electron donor and the electron acceptor, and the denominator takes into account the difference between the ionization potential  $I_{L\alpha}$  of the electron donor and the electron affinity  $A_{\beta^*}$  of the electron acceptor.  $I_{L\alpha}$  is increased by the predominantly positive electrostatic potential exerted on this atom by all the other molecules in the complex, whereas  $A_{\beta^*}$  is reduced by the predominantly negative electrostatic potential due to its surrounding ligands. The dependency of the denominator upon electrostatic potential and field effects was found essential to account for the strong nonadditive character of  $E_{\text{ct}}$  in polyligated  $\text{Zn}^{2+}$  complexes. The detailed expression for  $E_{\text{ct}}$  was given in refs 16 and 27.

$E_{\text{disp}}$  is the dispersion component, developed using the formulation of Creuzet et al.<sup>30</sup> and expressed as a sum of  $1/R^6$ ,  $1/R^8$ , and  $1/R^{10}$  terms at short distances by means of an exponential damping term. An explicit exchange-dispersion term is introduced for the mutual interactions between polyatomic molecules. Directionality effects are accounted for by the explicit introduction of fictitious atoms with reduced van der Waals radii to represent the lone pairs.

The fragment multipoles and polarizabilities were derived from ab initio computations using a double-dzeta valence basis set (DZVP2).<sup>31</sup> For the formate anion, the multipoles and polarizabilities were those derived from the CEP 4-31G(2d) basis of Stevens et al.<sup>32</sup> instead of the double-dzeta ones. This choice was adopted on the basis of subsequent comparisons between ab initio and SIBFA results (vide infra). For the perchlorate anion, the lone pair polarizabilities of each oxygen atom were relocated on the Cl–O bond to which the oxygen atom participates.

The intramolecular energy  $\Delta E_{\text{intra}}$  in a flexible molecule is computed as a sum of intermolecular interaction energies between the fragments making up the molecule, and use the same components and formulation as  $\Delta E_{\text{int}}$ .  $\Delta E_{\text{intra}}$  encompasses an additional torsional component,  $E_{\text{tor}}$ . The C–C and C–O torsional barriers were set to 2.3 and 1.5 kcal/mol, respectively, on the basis of ab initio computations on ethane and dimethyl ether.<sup>12</sup> Two-fold rotational barriers were used for rotations about bonds connecting the aromatic rings to their substituents, the corresponding  $E_{\text{tor}}$  minimum occurring when the substituent lies on the same plane as the aromatic ring. The minima were set values of –12, –9, and –20 kcal/mol for rotations about bonds connecting the C-amide to benzene, the N-amide to pyridine, and the O-methoxy to benzene. These values come from fits to ab initio conformational energy calculations on model amide- and methoxy-substituted benzene and pyridine compounds. Because we presently use the rigid rotor approximation, and in the absence of bond stretching and valence angle bending terms, the intramolecular energy of each isolated ligand or fragment is null.

The need for a simultaneous and consistent computation of inter- and intramolecular polarization and charge-transfer components because of their nonadditive character was recently emphasized.<sup>19,21,25,33</sup> To take these features into account, we have applied a new procedure tested on the intramolecular (conformational) energies of Ala tetrapeptides and validated by ab initio results (Gresh et al., manuscript in preparation), and recently applied in studies of a native and a mutated  $\text{Zn}^{2+}$  finger of the HIV-1 nucleocapsid.<sup>34</sup> As in the initial form of SIBFA,<sup>12</sup> the new procedure redistributes the multipoles at the junctions between fragments to compute  $E_{\text{MTP}}$ . On the other hand, to compute  $E_{\text{pol}}$ , the multipoles of the interfragment junctional

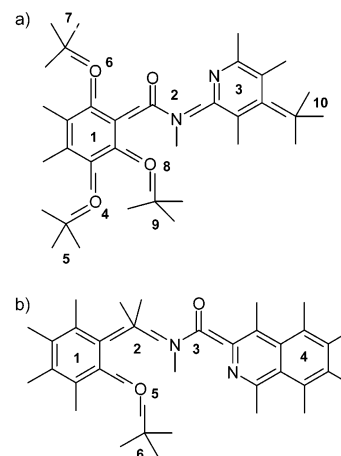


Figure 2. Constitutive fragments of (a) **L1** and (b) **L2**.

bonds are not redistributed, and the junctional H atoms are located on the C or N atoms whence they originate. This procedure prevents the fragments from acquiring a non-net fractional charge because of the multipole redistribution. It also prevents any junctional atom or bond multipole from being at too short distance ( $<1$  Å) from a polarizable center belonging to an adjacent fragment. The polarizabilities of the collapsed bonds are set to zero to prevent divergences of  $E_{\text{pol}}$  because of the effects of the induced dipoles.<sup>19,21</sup> Following this procedure, the ligand–ligand and ligand– $\text{Cu}^{2+}$  intermolecular interaction energies are computed as part of a global ‘intramolecular’ interaction that also encompasses the conformational energy variations of each of the flexible ligands.

In such cases, the complexation energy  $\Delta E_{\text{tot}}$  is computed as the difference between, on one hand, the global ‘intramolecular’ energy of the supermolecule made out of  $\text{Cu}^{2+}$ , and all its ligands, and, on the other hand, the summed intramolecular energies of optimized flexible ligands prior to complexation. The individual components of  $\Delta E_{\text{tot}}$  are, similarly, computed as the difference between their values in the complex and their corresponding sums in the isolated optimized ligands.

**L1** and **L2** were constructed using the multipoles and polarizabilities of their constitutive fragments. Thus, **L1** includes molecules of benzene (fragment 1), formamide (fragment 2), pyridine (fragment 3), water (fragments 4, 6, and 8), and methane (fragments 5, 7, 9, and 10), whereas **L2** includes benzene (fragment 1), methane (fragments 2 and 6), formamide (fragment 3), quinoline (fragment 4), and water (fragment 5) (Figure 2). Energy-minimizations on the complexes **C** and the ligands **L** were performed with the Merlin minimizer.<sup>35</sup>

To compare the relative stabilities of complexes **C** reported in Tables 7 and 8, we have completed the energy balances by including solvation effects. The stabilities of the complexes,  $\Delta E_{\text{stab}}$ , were calculated as follows (eq 2)

$$\Delta E_{\text{stab}} = E_{\text{C}} + E_{\text{solvC}} - 2(E_{\text{L}} + E_{\text{solvL}}) - 2E_{\text{solvX}} - E_{\text{solvCu}} \quad (2)$$

In eq 2,  $E_{\text{C}}$  denotes the total intramolecular energy of the complex consisting of each of the two ligands **L**,  $\text{Cu}^{2+}$ , and the two apical **X** ligands, namely water, methanol, or perchlorate ion.  $E_{\text{L}}$  denotes the total intramolecular energy of isolated ligand **L** in its energy-minimized conformation. The solvation energies (denoted as  $E_{\text{solv}}$ ) were computed using a Continuum reaction field procedure developed by Langlet et al.<sup>36</sup> and integrated in the SIBFA procedure.<sup>37</sup>  $E_{\text{solv}}$  is computed as a sum of five terms which are the electrostatic, repulsion, polarization, dispersion,



and cavitation components respectively (eq 3)

$$E_{\text{solv}} = E_{\text{MTP}} + E_{\text{rep}} + E_{\text{pol}} + E_{\text{disp}} + E_{\text{cav}} \quad (3)$$

Both electrostatic and polarization terms resort to the same distributed multipoles as in the SIBFA energy computations, which would thus ensure consistency between the two procedures. A multiplicative factor of the solute van der Waals surface of 1.2 was used. Accordingly, the exponent of the exponential intervening in  $E_{\text{rep}}$ , its multiplicative factor, as well as the multiplicative factor of  $E_{\text{disp}}$  were recalibrated in order to reproduce the solvation energies of small molecules. These values are 11.40, 28780, and 0.31.  $E_{\text{solvCu}}$  is evaluated as the sum of  $E(\text{Cu}(\text{H}_2\text{O})_6) + E_{\text{solv}}(\text{Cu}(\text{H}_2\text{O})_6) - 6E_{\text{solv}}(\text{H}_2\text{O})$ .

The energy-decompositions of the ab initio interaction energy were performed, at the HF level, using the CSOV procedure<sup>38</sup> interfaced in HONDO code<sup>39</sup> by one of us.<sup>40</sup> The CSOV, MP2, and DFT computations were done with the DZVP2 basis set.

We have reported as Supporting Information the  $\text{Cu}^{2+}$  parameters. These were fit in order to reproduce the values of the CSOV components of the ab initio interaction energies of this cation with water, imidazole, and methanethiolate, which were taken as representatives of O, N-, and S-containing ligands, respectively. In the present formulation of SIBFA, the electrostatic component  $E_{\text{MTP}}$  is intended to represent the pure “multipolar” component of its Coulomb CSOV counterpart and lacks its “penetration” part.<sup>41</sup> Therefore, and consistent with previous work,<sup>16</sup>  $E_{\text{rep}}$  was fit so that the sum of  $E_{\text{MTP}}$  and  $E_{\text{rep}}$ , denoted as  $E_1$ , reproduces its CSOV counterpart, namely the frozen core contribution which corresponds to the sum of Coulomb and exchange components.

As in our preceding studies, we have sought to first reproduce the individual terms of the HF interaction energy, consistent with our choice of uncorrelated multipoles and polarizabilities on the fragments. Therefore, to account in SIBFA for the gain in interaction energy that occurs upon passing to the correlated MP2 level, we resort to the actual  $E_{\text{disp}}$  component. However, the MP2 procedure is not a priori intended to account for actual dispersion effects. Inclusion of  $E_{\text{disp}}$  in its present form is therefore of a practical nature, whose usefulness can only be justified by its enabling to fit the correlation component  $E_{\text{cor}}$ . It cannot account for the nonadditivity properties of  $E_{\text{cor}}$ .<sup>20</sup>

In the computations bearing on rigid ligands (Tables 1–5), we have used the following notations:  $E_{\text{es}}$  and  $E_{\text{MTP}}$  denote, respectively, the QC Coulomb and the SIBFA electrostatic (multipolar) components of the interaction energy;  $E_{\text{ex}}$  and  $E_{\text{rep}}$  denote, similarly, the QC exchange and SIBFA short-range repulsion components;  $E_1$  is the sum of  $E_{\text{es}}$  and  $E_{\text{ex}}$  (QC) and of  $E_{\text{MTP}}$  and  $E_{\text{rep}}$  (SIBFA).  $E_{\text{pol}}$  and  $E_{\text{ct}}$  are the polarization and charge-transfer components from both QC and SIBFA approaches, the subscripts M or L denoting the cation and the ligands, respectively.  $E_2$  is the sum of  $E_{\text{pol}}$  and  $E_{\text{ct}}$ . We denote by  $\Delta E$  (without subscript) respectively the HF interaction energy in the QC computations (uncorrected for BSSE effects) and the SIBFA interaction energy prior to the inclusion of the dispersion energy component.  $E_{\text{cor}}$  denotes the QC interaction energy gain upon passing from the HF to the MP2 level, and  $E_{\text{disp}}$  denotes the SIBFA dispersion energy component. Finally,  $\Delta E_{\text{int}}$  denotes the total interaction energies upon adding  $E_{\text{cor/disp}}$  to  $\Delta E$ .

## Results and Discussion

Tables 1–5 report the results of test comparisons between SIBFA and quantum chemical calculations. Tables 1 and 2 report the results on monoligated complexes of  $\text{Cu}^{2+}$  with

**TABLE 1: Values (kcal/mol) of the Intermolecular Interaction Energies and Their Components in Complexes of  $\text{Cu}^{2+}$  with Neutral O and N Containing Ligands for the  $\text{Cu}^{2+}$  Ligand Distance  $d$  (given in Å) Optimized at the MP2 Level**

ligand	H <sub>2</sub> O		MeOH		HCOOH	
	ab initio	SIBFA	ab initio	SIBFA	ab initio	SIBFA
$E_{\text{es/MTP}}$	−93.0	−73.1	−94.7	−68.0	−98.2	−87.4
$E_{\text{ex/rep}}$	50.8	25.8	51.7	26.6	53.9	33.5
$E_1$	−42.2	−47.3	−43.0	−41.1	−44.3	−53.9
$E_{\text{pol(M)}}$	−1.8	−0.8	−1.0	−0.9	−2.9	−1.3
$E_{\text{ct(M)}}$	−0.8		−0.8		−1.3	
$E_{\text{pol(L)}}$	−25.7	−27.8	−37.9	−38.2	−66.3	−53.9
$E_{\text{ct(L)}}$	−6.3	−7.8	−6.8	−7.3	−6.0	−9.1
$E_2$	−34.4	−35.8	−41.8	−45.5	−77.6	−64.5
$\Delta E$	−80.5	−83.0	−91.0	−86.9	−123.7	−118.4
$E_{\text{cor/disp}}$	−2.7	−4.8	−5.0	−6.4	−3.5	−7.2
$\Delta E_{\text{int}}$	−83.2	−87.8	−96.0	−93.3	−127.2	−125.6
$d$ (Å)	1.9		1.9		1.8	

ligand	HCONH <sub>2</sub>		ImH		pyridine	
	ab initio	SIBFA	ab initio	SIBFA	ab initio	SIBFA
$E_{\text{es/MTP}}$	−128.7	−94.3	−140.4	−106.7	−131.3	−95.0
$E_{\text{ex/rep}}$	62.9	30.1	78.0	41.5	83.9	42.0
$E_1$	−65.7	−64.2	−62.4	−65.1	−47.4	−53.0
$E_{\text{pol(M)}}$	−1.6	−1.2	−3.7	−2.8	−4.0	−2.7
$E_{\text{ct(M)}}$	−1.3		−1.2		−1.2	
$E_{\text{pol(L)}}$	−65.3	−65.7	−76.3	−82.1	−81.2	−82.1
$E_{\text{ct(L)}}$	−6.3	−7.5	−7.1	−13.9	−9.6	−13.8
$E_2$	−76.2	−73.2	−88.3	−95.9	−98.5	−98.7
$\Delta E$	−143.9	−137.4	−156.6	−161.0	−150.4	−151.5
$E_{\text{cor/disp}}$	−2.9	−6.9	−10.6	−9.5	−13.0	−10.2
$\Delta E_{\text{int}}$	−146.8	−144.4	−167.2	−170.3	−163.6	−161.8
$d$ (Å)	1.8		1.9		1.9	
$\Delta E_{\text{int}}^a$		−147.2				
$d$ (Å) <sup>b</sup>		1.7				

<sup>a</sup> Value obtained for the SIBFA optimized distance when different from ab initio. <sup>b</sup> SIBFA optimized distance.

neutral (O and N) and anionic (O and S) ligands, respectively. Table 3 reports the results on representative polyligated complexes of  $\text{Cu}^{2+}$  with neutral ( $\text{H}_2\text{O}$ ) as well as anionic (formate, perchlorate) ligands, whereas Table 4 reports the results on two representative binuclear  $\text{Cu}^{2+}$  complexes with formate and water. Table 5 bears on the complexes of  $\text{Cu}^{2+}$  bound to two truncated models of ligands **L1** and **L2** and two formate ions. A comparison of the structural features of  $\text{Cu}^{2+}$  complexes **C1** and **C2** respectively obtained by X-ray diffraction and by SIBFA optimization is described in Table 6. Tables 7 and 8 report the results of the SIBFA calculations on  $\text{Cu}^{2+}$  complexes formed respectively from acetate ions and from the **L1** and **L2** ligands and their derivatives.

**1. Monoligated Complexes of  $\text{Cu}^{2+}$ .** In all of the complexes considered,  $\text{Cu}^{2+}$  remains in its dicationic form, that is, no electron transfer takes place from the ligand to  $\text{Cu}^{2+}$  that would result into two interacting monocations. However, in the case of water, the first evidence for an  $(\text{H}_2\text{O})^+-\text{M}^+$  complex energetically more favorable than  $(\text{H}_2\text{O})-\text{M}^{2+}$  was shown in the case of  $\text{Mg}^{2+}$  by Corongiu and Clementi.<sup>42</sup> Similarly, recent CCSD(T) and DFT computations by El-Nahas et al.<sup>43</sup> which bore on the complexes of  $\text{Cu}^{2+}$  with  $\text{H}_2\text{O}$  and  $\text{NH}_3$ , showed the  $\text{L}^+-\text{Cu}^+$  form to be more stable, at increased cation–ligand separation, than the  $\text{L}-\text{M}^{2+}$  one at equilibrium distance. However, the latter complex was separated from the former by an energy barrier whose magnitude increased upon increasing the number of ligands, which should result in the prevalence of the “dicationic Cu” form upon progressive completion of the first-shell cation ligation shell. In this connection, recent mass

**TABLE 2: Values (kcal/mol) of the Intermolecular Interaction Energies and Their Components in the Complexes of Cu<sup>2+</sup> with O and S Containing Anionic Ligands for the Cu<sup>2+</sup> Ligand Distance *d* Optimized at the MP2 Level**

ligand	OH <sup>-</sup>		CH <sub>3</sub> S <sup>-</sup>		HCOO <sup>-</sup>			
					monodentate		bidentate	
	ab initio	SIBFA	ab initio	SIBFA	ab initio	SIBFA	ab initio	SIBFA
<i>E</i> <sub>es/MTP</sub>	-438.9	-381.9	-361.5	-331.0	-359.5	-308.4	-381.0	-337.8
<i>E</i> <sub>ex/rep</sub>	119.9	64.7	99.3	63.7	118.1	58.8	89.8	53.0
<i>E</i> <sub>1</sub>	-319.0	-317.2	-262.1	-267.4	-241.4	-249.6	-291.2	-284.9
<i>E</i> <sub>pol(M)</sub>	-5.0	-6.4	-1.6	-5.8	-6.0	-4.9	-3.6	-1.1
<i>E</i> <sub>ct(M)</sub>	-2.0		-1.0		-1.7		-1.5	
<i>E</i> <sub>pol(L)</sub>	-56.2	-72.5	-46.3	-69.0	-72.0	-70.7	-66.5	-73.4
<i>E</i> <sub>ct(L)</sub>	-11.4	-11.6	-54.6	-42.6	-10.8	-12.7	-17.8	-19.5
<i>E</i> <sub>2</sub>	-75.6	-84.1	-103.7	-111.6	-93.2	-83.4	-89.9	-92.9
<b>Δ<i>E</i></b>	<b>-400.1</b>	<b>-401.3</b>	<b>-380.0</b>	<b>-379.0</b>	<b>-337.9</b>	<b>-333.1</b>	<b>-385.4</b>	<b>-377.7</b>
<i>E</i> <sub>cor/disp</sub>	-10.6	-11.3	-22.5	-26.7	-14.0	-9.7	-13.5	-11.0
<b>Δ<i>E</i><sub>int</sub></b>	<b>-410.7</b>	<b>-413.0</b>	<b>-402.5</b>	<b>-405.6</b>	<b>-351.9</b>	<b>-342.8</b>	<b>-398.9</b>	<b>-388.8</b>
<i>d</i> (Å)	1.7		2.2		1.7		2.0	

ligand	ClO <sub>4</sub> <sup>-</sup>			
	monodentate		bidentate	
	ab initio	SIBFA	ab initio	SIBFA
<i>E</i> <sub>es/MTP</sub>	-239.0	-217.5	-286.9	-250.7
<i>E</i> <sub>ex/rep</sub>	57.9	29.4	85.5	36.6
<i>E</i> <sub>1</sub>	-181.2	-181.8	-201.4	-214.0
<i>E</i> <sub>pol(M)</sub>	-1.8	-1.1	-1.4	-1.6
<i>E</i> <sub>ct(M)</sub>	-1.5		-1.6	
<i>E</i> <sub>pol(L)</sub>	-68.0	-46.9	-74.5	-78.1
<i>E</i> <sub>ct(L)</sub>	-6.7	-11.4	-18.9	-17.7
<i>E</i> <sub>2</sub>	-81.1	-58.3	-97.0	-95.9
<b>Δ<i>E</i></b>	<b>-265.7</b>	<b>-240.1</b>	<b>-301.5</b>	<b>-309.9</b>
<i>E</i> <sub>cor/disp</sub>	-18.0	-8.8	-22.3	-18.7
<b>Δ<i>E</i><sub>int</sub></b>	<b>-283.7</b>	<b>-248.8</b>	<b>-323.8</b>	<b>-328.5</b>
<i>d</i> (Å)	1.8		2.0	
<i>E</i> <sub>int</sub> <sup>a</sup>				-336.5
<i>d</i> (Å) <sup>b</sup>				1.86

<sup>a,b</sup> As in Table 1.**TABLE 3: Values (kcal/mol) of the SIBFA and HF, MP2, and B3LYP Intermolecular Interaction Energies in Polyligated Complexes of Cu<sup>2+</sup> with Neutral and Anionic Ligands**

ligands	(H <sub>2</sub> O) <sub>6</sub>	(H <sub>2</sub> O) <sub>5</sub> (H <sub>2</sub> O)	[(HCOO) <sup>-</sup> ] <sub>2</sub>	[(HCOO) <sup>-</sup> ] <sub>2</sub> (H <sub>2</sub> O) <sub>2</sub>	[(ClO <sub>4</sub> ) <sup>-</sup> ] <sub>2</sub> (H <sub>2</sub> O) <sub>4</sub>	
					direct	through water
<i>E</i> <sub>MTP</sub>	-333.8	-323.3	-559.1	-632.5	-591.3	-567.1
<i>E</i> <sub>rep</sub>	85.3	95.0	71.0	102.1	110.7	110.6
<i>E</i> <sub>1</sub>	-248.5	-228.3	-488.2	-530.4	-480.6	-456.5
<i>E</i> <sub>pol(M)</sub>	0.0	0.0	0.0	-0.1	0.0	-0.2
<i>E</i> <sub>pol(L)</sub>	-61.0	-71.6	-80.7	-73.8	-72.8	-82.2
<i>E</i> <sub>ct(L)</sub>	-11.6	-13.7	-16.0	-16.0	-13.4	-15.5
<i>E</i> <sub>2</sub>	-72.6	-85.3	-96.7	-79.8	-86.2	-97.9
<b>Δ<i>E</i><sub>SIBFA</sub></b>	<b>-321.1</b>	<b>-313.7</b>	<b>-584.8</b>	<b>-620.3</b>	<b>-566.8</b>	<b>-554.4</b>
<b>Δ<i>E</i><sub>HF</sub></b>	<b>-321.3</b>	<b>-321.9</b>	<b>-593.0</b>	<b>-625.5</b>	<b>-572.1</b>	<b>-561.0</b>
<i>E</i> <sub>disp</sub>	-28.3	-27.3	-18.4	-28.2	-48.1	-45.1
<b>Δ<i>E</i><sub>int</sub>-SIBFA</b>	<b>-349.4</b>	<b>-340.9</b>	<b>-603.2</b>	<b>-648.4</b>	<b>-614.8</b>	<b>-599.5</b>
<b>Δ<i>E</i><sub>MP2</sub></b>	<b>-352.8</b>	<b>-351.3</b>	<b>-618.5</b>	<b>-654.0</b>	<b>-630.2</b>	<b>-613.9</b>
<b>Δ<i>E</i><sub>B3LYP</sub></b>	<b>-361.4</b>	<b>-368.0</b>	<b>-658.0</b>	<b>-679.9</b>	<b>-626.9</b>	<b>-617.9</b>
<b>Δ<i>E</i><sub>opt</sub>-B3LYP</b>	<b>-366.4</b>	<b>-373.1</b>	<b>-667.2</b>	<b>-696.6</b>	<b>-639.8</b>	<b>-641.1</b>

spectrometry experiments indicated the prevalence of the “dicationic Cu” form when the number of ligands increased to 3, such as in [Cu.(H<sub>2</sub>O)<sub>3</sub>]<sup>2+</sup> or [Cu.(NH<sub>3</sub>)<sub>3</sub>]<sup>2+</sup>.<sup>44</sup> The present CSOV computations on monoligated complexes detect solely the dicationic Cu<sup>2+</sup> form, which is the relevant one for simulations of the polyligated complexes of divalent cations. It is therefore these calculations that will serve as a benchmark for SIBFA. For the latter, it is noted that the reduction occurring, in the denominator of *E*<sub>ct</sub> of *A*<sub>β\*</sub>, by the potential that Cu<sup>2+</sup> undergoes stemming from its ligands, along with the concomitant increase of *I*<sub>Lα</sub> of the ligands by the predominantly positive potential undergone by each, results in a positive denominator in the range of Cu–L distances of interest (by up to 0.8 Å away

from equilibrium distance), and that such a range is increased upon progressive build-up of the first ligation shell.

**Neutral Ligands.** In addition to water, the ligands investigated are Cu<sup>2+</sup>-binding moieties encountered in the protein main-chains (formamide), side-chains (methanol for Ser or Thr, formamide for Asn or Gln, imidazole (ImH) for His, as well as formic acid for protonated Asp or Glu side-chains), or in supramolecular chemistry (pyridine). *ΔE*<sub>int</sub>(SIBFA) is seen from the values reported in Table 1 to reproduce closely *ΔE*<sub>int</sub>(MP2). Within the HF and SIBFA approaches, the second-order term *E*<sub>2</sub> has large magnitudes, due essentially to *E*<sub>pol</sub>(L). It is noteworthy that in most investigated complexes excepting water and methanol, and for both ab initio and SIBFA computations,

**TABLE 4: Values (kcal/mol) of the SIBFA and HF, MP2, and B3LYP Intermolecular Interaction Energies in the Complexes between Two Cu<sup>2+</sup> Cations and Four Formate Anions and between Two Cu<sup>2+</sup> Cations and Four Formate Anions and Two Water Molecules**

ligands	(HCOO <sup>-</sup> ) <sub>4</sub>	(HCOO <sup>-</sup> ) <sub>4</sub> (H <sub>2</sub> O) <sub>2</sub>
$E_{\text{MTP}}$	-1242.8	-1310.8
$E_{\text{rep}}$	177.3	191.8
$E_1$	1065.45	-1118.9
$E_{\text{pol}}(\text{M})$	-1.0	0.0
$E_{\text{pol}}(\text{L})$	-130.3	-117.9
$E_{\text{ct}}(\text{L})$	-30.6	-27.6
$E_2$	-160.9	-145.4
$\Delta E_{\text{SIBFA}}$	<b>-1226.4</b>	<b>-1264.4</b>
$\Delta E_{\text{HF}}$	<b>-1200.0</b>	<b>-1275.3</b>
$E_{\text{disp}}$	-56.8	-65.5
$\Delta E_{\text{int-SIBFA}}$	<b>-1283.1</b>	<b>-1329.9</b>
$\Delta E_{\text{MP2}}$	<b>-1252.6</b>	<b>-1348.1</b>
$\Delta E_{\text{B3LYP}}$	-1364.0	-1385.8
$\Delta E_{\text{(opt-B3LYP)}}$	<b>-1368.7</b>	<b>-1391.5</b>

**TABLE 5: Interaction Energy Values (kcal/mol) in Truncated C1 and C2 Complexes with Apical Formate Anions**

in plane ligands	C1a trans	C1a cis	C2a trans	C2a cis
$E_{\text{MTP}}$	-634.2	-663.9	-626.3	-652.4
$E_{\text{rep}}$	103.0	117.4	103.7	112.6
$E_1$	-531.2	-546.5	-517.6	-539.7
$E_{\text{pol}}$	-83.6	-65.6	-91.3	-54.8
$E_{\text{ct}}$	-16.4	-10.9	-17.2	-10.8
$E_2$	-99.9	-76.5	-108.5	-65.6
$\Delta E_{\text{SIBFA}}^a$	-631.2	-623.0	-626.1	-605.3
$E_{\text{tor}}$	3.2	-2.1	6.4	1.8
$\Delta E_{\text{SIBFA}}^b$	<b>-628.0</b>	<b>-625.1</b>	<b>-619.7</b>	<b>-603.5</b>
$\Delta E(\text{HF})^c$	<b>-640.1</b>	<b>-624.2</b>	<b>-623.7</b>	<b>-614.7</b>
$E_{\text{disp}}$	-44.7	-51.6	-47.2	-46.8
$\Delta E_{\text{tot-SIBFA}}$	<b>-672.7</b>	<b>-676.8</b>	<b>-666.9</b>	<b>-650.3</b>
$\Delta E(\text{DFT})^c$	-705.9	-678.9	-692.6	-673.6
$\Delta E(\text{DFT})^d$	<b>-703.5</b>	<b>-682.2</b>	<b>-694.5</b>	<b>-677.6</b>

<sup>a</sup> In the absence of both dispersion and 2-fold torsional energy components. <sup>b</sup> In the absence of the dispersion energy component. <sup>c</sup> Interaction energies computed at the SIBFA minima. <sup>d</sup> Interaction energies minimized by DFT.

$E_2$  has a larger magnitude than  $E_1$ . This feature is more pronounced in the case of the pyridine-Cu<sup>2+</sup> complex.

**Anionic Ligands.** Among the ligands investigated, methanethiolate and formate, which correspond to the terminal fragments of the side-chains of deprotonated Cys and Asp/Glu side-chains respectively, are widely encountered Cu-ligands in proteins. Several data have suggested the possible involvement of OH<sup>-</sup> as a ligand for transition-metal dications in the active site of metalloenzymes after the deprotonation of a water molecule.<sup>45</sup> The perchlorate anion is a common counterion used in crystallization and extraction studies, and it was deemed important to include it into the present survey.

For the complexes of Cu<sup>2+</sup> with OH<sup>-</sup>, methanethiolate, as well as formate, we see from Table 2 that  $\Delta E_{\text{int}}(\text{SIBFA})$  affords a close match to  $\Delta E_{\text{int}}(\text{MP2})$ , the relative error being inferior to 3%. The relative magnitudes within  $\Delta E$  of the ab initio  $E_1$  and  $E_2$  components are correctly reflected by the SIBFA calculations. Noteworthy is the very large magnitude of  $E_{\text{ct}}$  in the Cu<sup>2+</sup>-CH<sub>3</sub>S<sup>-</sup> complex. Such a numerical value is fully consistent with those found in the related complex of CH<sub>3</sub>S<sup>-</sup> with Zn<sup>2+</sup>.<sup>16</sup> The trends of  $\Delta E_{\text{int}}(\text{MP2})$  upon passing from monodentate to bidentate Cu<sup>2+</sup> binding in the formate complex are accounted for. For the Cu<sup>2+</sup> complex with perchlorate, however, although  $\Delta E_{\text{int}}(\text{SIBFA})$  in the bidentate complex closely reproduces  $\Delta E_{\text{int}}(\text{MP2})$ , it provides a less satisfactory

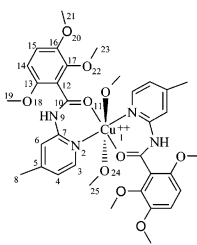
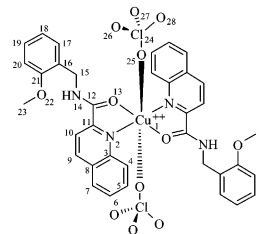
match in the monodentate complex. In this case,  $\Delta E_{\text{int}}(\text{SIBFA})$  is smaller by 9% than  $\Delta E_{\text{int}}(\text{MP2})$ . Examination of the components of  $\Delta E$  shows this to stem from  $E_{\text{pol}}(\text{SIBFA})$ . As mentioned in the Procedure section, the polarizabilities of the perchlorate anion, initially distributed on four Cl-O bonds and the lone pairs of the anionic O atoms, were relocated on the sole four Cl-O bonds to avoid the loss of rotational invariance. Alternative relocations may be necessary in order to obtain a better representation of  $E_{\text{pol}}$  in a diversity of ClO<sub>4</sub><sup>-</sup> complexes if more extensive simulations concerning this anion were necessary.

**2. Polyligated Complexes.** A very important issue upon passing from mono- to polyligated complexes of divalent cations relates to the very strong nonadditive characters of the second-order components of the interaction energy,  $E_{\text{pol}}$  and  $E_{\text{ct}}$ , as well as of the correlation energy. This has been shown in several studies on Zn<sup>2+</sup> polyligated complexes.<sup>17,20</sup> However, an evaluation of the amount of nonadditivities of  $E_{\text{pol}}$  and  $E_{\text{ct}}$  cannot be obtained for open-shell systems, because the code that we use here can handle only two entities. This implies that the different ligands have to be treated as a single molecule. An additional complication with respect to closed-shell cations relates to the onset of ligand field effects on the singly occupied 3d Cu<sup>2+</sup> orbital. Nevertheless, the comparisons between the total energies, both uncorrelated and correlated, with the corresponding SIBFA ones should be instructive.

We have compared SIBFA and QC results for small model complexes of Cu<sup>2+</sup>. This was first done with neutral ligands, as represented by water molecules. For  $n = 6$  waters, we have thus investigated the dependence of the interaction energy upon the number of solvating first-shell molecules, namely from 4 to 6. As models for anionic ligands, we resorted to formate and perchlorate. Although the first is encountered in a diversity of biologically and pharmacologically important molecules, the second is frequently used as a counterion in Cu<sup>2+</sup> solutions, so that it could be important to have a good representation of ClO<sub>4</sub><sup>-</sup> for prospective simulations of Cu<sup>2+</sup> complexes in solution.

The first observation relates to the close matches of  $\Delta E_{\text{int}}(\text{SIBFA})$  (without the  $E_{\text{disp}}$  term) and  $\Delta E(\text{HF})$  values at the corresponding geometries, the relative errors being for all investigated complexes inferior to 2.5% as can be seen from the values of Table 3. On the other hand, however, the quantum chemical computations give differing results upon passing from the uncorrelated to the correlated levels, according to the computational method, MP2 or DFT. The energy gains due to correlation are smaller at the MP2 than at the DFT level. This was already noted in studies of the binuclear complexes of Cu<sup>+</sup> with imidazole ligands in models of the native form of tyrosinase/hemocyanin.<sup>22</sup> The results of El-Nahas et al. on small mono- and biligated complexes of Cu<sup>2+</sup> gives, with CCSD(T), interaction energies smaller than the B3LYP methodology, but closer to the MP2 ones in the case of monoligated Cu<sup>2+</sup> complexes. This could imply that in the case of the larger polyligated complexes investigated here, which are not amenable to CCSD(T) computations, the present MP2 results should represent a closer approximation to CCSD(T) than DFT. This should justify the calibration of  $E_{\text{disp}}(\text{SIBFA})$  in order to reproduce  $E_{\text{cor}}$  from MP2 rather than from DFT.  $\Delta E_{\text{int}}(\text{SIBFA})$  has values closer to the MP2 than to the DFT ones. An explicit representation of ligand field effects could provide a more accurate reproduction of the trends from QC calculations. Thus, in Cu<sup>2+</sup> (H<sub>2</sub>O)<sub>6</sub> (Figure 3a), in the SIBFA-optimized geometry, all six Cu-O distances are identical (2.13 Å), whereas from the quantum chemical ones taking into account correlation, a

**TABLE 6: Comparison of the C1 and C2 Distances (Å) Angles (°) and Dihedrals (°) Minimized with the SIBFA Procedure with the Ones Obtained by Crystallography (ESD Mentioned in Parentheses)**

	Crystallography		SIBFA		
<b>C1</b>					
	O <sub>11</sub> -Cu <sub>1</sub>	1.955(1)	1.91	1.90	
	N <sub>2</sub> -Cu	2.011(2)	2.14	2.15	
	Cu <sub>1</sub> -O <sub>24</sub>	2.423(2)	2.09	2.14	
	O <sub>11</sub> -Cu <sub>1</sub> -N <sub>2</sub>	89.17(6)	85.72	85.94	
	O <sub>11</sub> -Cu <sub>1</sub> -N <sub>2</sub> #	90.83(6)	93.70	94.69	
	O <sub>11</sub> -Cu <sub>1</sub> -O <sub>24</sub>	90.11(8)	94.51	95.08	
	N <sub>2</sub> -Cu <sub>1</sub> -O <sub>24</sub>	86.56(8)	90.82	92.19	
	C <sub>21</sub> -O <sub>20</sub> -C <sub>16</sub> -C <sub>15</sub>	7.6(4)	-7.6(4)#	26.78	-28.58
	C <sub>23</sub> -O <sub>22</sub> -C <sub>17</sub> -C <sub>16</sub>	76.3(3)	-76.3(3)#	56.63	-62.15
	C <sub>19</sub> -O <sub>18</sub> -C <sub>13</sub> -C <sub>12</sub>	17.4(2)	-17.4(2)#	32.05	-30.56
O <sub>11</sub> -C <sub>10</sub> -C <sub>12</sub> -C <sub>13</sub>	117.0(2)	-117.0(2)#	129.77	-131.16	
C <sub>10</sub> -N <sub>9</sub> -C <sub>7</sub> -C <sub>6</sub>	-164.7(2)	164.7(2)#	-174.09	172.65	
<b>C2</b>					
	O <sub>13</sub> -Cu <sub>1</sub>	1.924(2)	1.92	1.93	
	N <sub>2</sub> -Cu <sub>1</sub>	2.097(2)	2.26	2.22	
	Cu <sub>1</sub> -O <sub>25</sub>	2.464(8)	2.21	2.20	
	O <sub>13</sub> -Cu <sub>1</sub> -N <sub>2</sub>	80.85(7)	79.67	79.97	
	O <sub>13</sub> -Cu <sub>1</sub> -N <sub>2</sub> #	99.15(7)	101.70	98.74	
	O <sub>13</sub> -Cu <sub>1</sub> -O <sub>25</sub>	78.01(8)	91.23	87.48	
	N <sub>2</sub> -Cu <sub>1</sub> -O <sub>25</sub>	94.06(8)	92.39	97.80	
	C <sub>20</sub> -C <sub>21</sub> -O <sub>22</sub> -C <sub>23</sub>	0.4(5)	-0.4(5)#	-3.36	33.06
	N <sub>14</sub> -C <sub>15</sub> -C <sub>16</sub> -C <sub>17</sub>	87.3(3)	-87.3(3)#	87.70	-87.99
	C <sub>10</sub> -C <sub>11</sub> -C <sub>12</sub> -N <sub>14</sub>	2.5(3)	-2.5(3)#	21.17	-16.71
C <sub>12</sub> -N <sub>14</sub> -C <sub>15</sub> -C <sub>16</sub>	-95.8(3)	95.8(3)#	-101.78	103.98	

<sup>a</sup> Symmetry-related crystallographic data.

**TABLE 7: Values (kcal/mol) of the SIBFA Interaction Energy in Complexes C1, C2 and in the Cu<sup>2+</sup> Complexes with One or Two Acetate Ions**

com- plexes			Cu(OAc) <sub>2</sub> (H <sub>2</sub> O) <sub>4</sub>		
	C1	C2	[CuOAc(H <sub>2</sub> O) <sub>5</sub> ] <sup>+</sup>	CN = 5	CN = 6
<i>E</i> <sub>MTP</sub>	-397.3	-353.7	-544.4	-648.7	-665.4
<i>E</i> <sub>rep</sub>	120.2	105.5	104.1	122.9	108.9
<i>E</i> <sub>pol</sub>	-126.2	-129.1	-75.7	-93.7	-70.4
<i>E</i> <sub>ct</sub>	-11.6	-10.4	-15.6	-22.0	-14.4
<i>E</i> <sub>disp</sub>	-46.3	-45.1	-34.8	-36.4	-38.7
<b>Δ<i>E</i><sub>int</sub></b>	<b>-460.5</b>	<b>-432.5</b>	<b>-566.4</b>	<b>-677.8</b>	<b>-679.9</b>
<i>E</i> <sub>tor</sub>	-11.3	2.9	0.0	0.0	0.0
<i>E</i> <sub>solv</sub>	-110.3	-127.2	4.6	107.9	110.5
<b>Δ<i>E</i><sub>stab</sub><sup>a</sup></b>	<b>-34.9</b>	<b>-9.8</b>	<b>-3.0</b>	<b>-14.9</b>	<b>-14.5</b>

<sup>a</sup> *E*<sub>solvCu</sub> = -539.2 kcal/mol; *E*<sub>solvW</sub> = -3.9 kcal/mol.

slight elongation of the two axial Cu-O distances with respect to the two apical ones is obtained (2.20 versus 2.10 Å). The complex Cu<sup>2+</sup>(H<sub>2</sub>O)<sub>5</sub>(H<sub>2</sub>O) (Figure 3b), having one outer-shell water molecule, is 8.5 kcal/mol less stable than the Cu<sup>2+</sup>(H<sub>2</sub>O)<sub>6</sub>, consistent with the corresponding results found for Zn<sup>2+</sup> by both SIBFA and ab initio MP2 computations.<sup>20</sup> In the case of Cu<sup>2+</sup>, on the other hand, HF, DFT, and MP2 all give Cu<sup>2+</sup>-(H<sub>2</sub>O)<sub>5</sub>(H<sub>2</sub>O) to be isoenergetic with, or slightly more stable than, Cu<sup>2+</sup>(H<sub>2</sub>O)<sub>6</sub>.

**TABLE 8: Values (kcal/mol) of the SIBFA Interaction Energy in the C1 Derivatives**

com- plexes	C1	C1b	C1c	C1d	C1e	C1f	C1g
<i>E</i> <sub>MTP</sub>	-397.3	-363.1	-363.6	-370.3	-390.1	-375.2	-393.3
<i>E</i> <sub>rep</sub>	120.2	100.3	103.2	104.9	116.3	110.7	112.7
<i>E</i> <sub>pol</sub>	-126.2	-122.5	-125.6	-128.6	-122.1	-128.4	-127.2
<i>E</i> <sub>ct</sub>	-11.6	-11.2	-11.5	-11.2	-11.7	-11.3	-11.5
<i>E</i> <sub>disp</sub>	-46.3	-40.3	-41.9	-41.4	-45.7	-42.1	-44.6
<b>Δ<i>E</i><sub>int</sub></b>	<b>-460.5</b>	<b>-436.4</b>	<b>-438.9</b>	<b>-446.1</b>	<b>-453.0</b>	<b>-445.8</b>	<b>-463.1</b>
<i>E</i> <sub>tor</sub>	-11.3	-2.0	-2.8	-5.4	-6.3	-7.1	-6.2
<i>E</i> <sub>solv</sub>	-110.3	-132.5	-133.3	-124.8	-115.3	-124.4	-110.5
<b>Δ<i>E</i><sub>stab</sub><sup>a</sup></b>	<b>-34.9</b>	<b>-23.8</b>	<b>-22.4</b>	<b>-29.1</b>	<b>-28.4</b>	<b>-30.3</b>	<b>-32.8</b>
<i>E</i> <sub>MTP**b</sub>	-142.4	-127.7	-130.3	-131.7	-139.2	-132.9	-142.2

<sup>a</sup> *E*<sub>solvCu</sub> = -539.2 kcal/mol; *E*<sub>solvW</sub> = -3.9 kcal/mol. <sup>b</sup> The C1 derivatives were constructed with a +1 charge for Cu and without apical water molecules.

Two complexes with two formate anions were considered, the second one having two additional water molecules. In the absence of waters, Cu<sup>2+</sup> is bound bidentate to the two formates, so that its coordination number is four (CN = 4). In the second complex, Cu<sup>2+</sup>(HCOO<sup>-</sup>)<sub>2</sub>(H<sub>2</sub>O)<sub>2</sub> (Figure 3c), Cu<sup>2+</sup> is bound monodentate to each formate anion and bound to each water as well and, thus, also has a coordination number of four. Each water is hydrogen bonded to the Cu-unbound anionic oxygen of one formate. Some shortcomings of the use of fixed internal



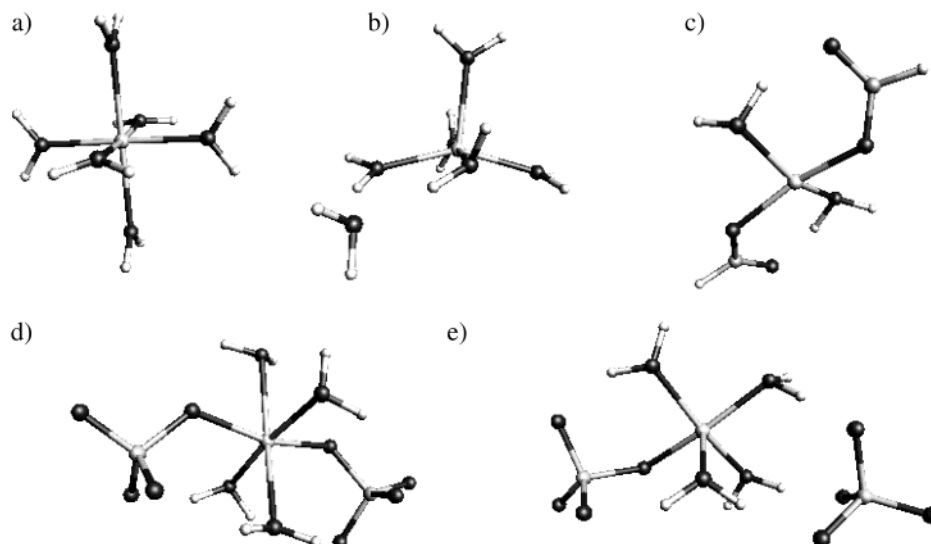


**Figure 3.** Optimized arrangements of the following complexes: (a)  $[\text{Cu}(\text{H}_2\text{O})_6]^{2+}$ ; (b)  $[\text{Cu}(\text{H}_2\text{O})_5(\text{H}_2\text{O})]^{2+}$ ; (c)  $\{\text{Cu}^{2+}[(\text{HCOO})_2]^{2-} (\text{H}_2\text{O})_2\}$ ; (d)  $\{\text{Cu}^{2+}[(\text{ClO}_4)_2]^{2-} (\text{H}_2\text{O})_4\}$  with direct binding of  $\text{Cu}^{2+}$  to both perchlorate anions; (e)  $\{\text{Cu}^{2+}[(\text{ClO}_4)_2]^{2-} (\text{H}_2\text{O})_4\}$  with direct binding of  $\text{Cu}^{2+}$  to one perchlorate anion and through-water binding to the other.

geometries in the SIBFA computations on perchlorate anions occur in the case of the complexes of  $\text{Cu}^{2+}$  with two perchlorate anions and four waters. Thus, a “direct” binding of both  $\text{ClO}_4^-$  anions through one O atom (Figure 3d) is predicted to be more favorable than an alternative mode in which one anion binds  $\text{Cu}^{2+}$  through one water molecule (Figure 3e). This is consistent with the results from single-point calculations with HF, DFT, and MP2 approaches. However, DFT energy-minimizations result in the through-water binding mode being slightly more favorable than the direct binding mode. Such a difference is most probably due to a 0.08 Å lengthening of the Cl–O distances involving the  $\text{Cu}^{2+}$ -coordinating O atoms, whereas the SIBFA computations retain a 1.51 Å bond length for all Cl–O bonds.

**3. Binuclear Complexes.** Binuclear complexes of copper with at least one dipositive  $\text{Cu}^{2+}$  cation are found within the active site of cytochrome C oxidase.<sup>46</sup> In addition, hetero-binuclear complexes of two divalent cations involving one  $\text{Cu}^{2+}$  cation are found in several metalloenzymes, such as Zn(II)/Cu(II) superoxide dismutase, etc.<sup>47</sup> In view of our interest in simulations of the active site of binuclear metalloenzymes<sup>20</sup> and their complexes with inhibitors,<sup>25</sup> we wished to evaluate how well SIBFA would reproduce the QC results, considering the very substantial increases of the magnitudes of the interaction energies. We have reported in Table 4 the results for the complexes formed between: two  $\text{Cu}^{2+}$  cations and (a) four formate anions; (b) four formate anions and two water molecules. The latter arrangement is represented in Figure 4.

With respect to the mononuclear complex  $\text{Cu}^{2+}(\text{HCOO}^-)_2$ , for which  $\Delta E_{\text{int}}$  is equal to –603.2, –618.5, and –658.0 kcal/mol from SIBFA, MP2, and DFT, respectively, the interaction energies in  $[\text{Cu}^{2+}(\text{HCOO}^-)_2]_2$  are multiplied by a factor slightly larger than 2, namely 2.02–2.07 in the quantum chemical computations and 2.13 in the SIBFA ones. This is indicative of attractive interactions between the two mononuclear entities, in contrast to the strong anticooperative character of the binuclear complexes of  $\text{Zn}^{2+}$  in Gal4 and  $\beta$ -lactamase models.<sup>20</sup>  $\Delta E(\text{SIBFA})$  reproduces  $\Delta E(\text{HF})$  values with relative errors of 2.5%. At the correlated level, as for mononuclear and binuclear  $\text{Cu}^+$  complexes with imidazoles,<sup>22</sup>  $\Delta E(\text{MP2})$  has smaller values than  $\Delta E(\text{DFT})$ , with  $\Delta E_{\text{int}}(\text{SIBFA})$  being intermediate between them. DFT-energy-minimization results into interaction energy

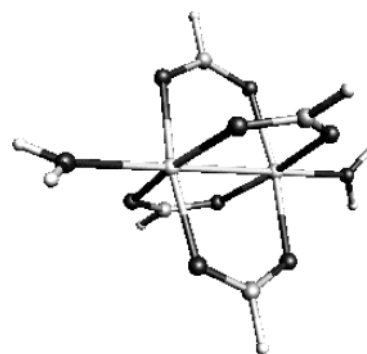


**Figure 4.** Optimized arrangement of the  $\{\text{Cu}^{2+}[(\text{HCOO})_2]^{2-} (\text{H}_2\text{O})_2\}_2$  complex.

gains of 4–6 out of 1350 kcal/mol with respect to the SIBFA-minimized structure.

**4. Truncated Models of C1 and C2.** For comparison with quantum chemical computations, we have used simplified models of complexes **C1** and **C2**. For the first model **C1a**, **L1** was replaced by pyridine ortho-substituted with methylformamide through the *N*-amide, whereas for the second model **C2a**, **L2** was replaced by pyridine ortho-substituted with methylformamide through the carbonyl *C*-amide. Both complexes have formate as apical ligands. Two distinct binding arrangements were considered (Figure 5). In the first, denoted as *trans*, the C=O bond is in a *trans* conformation with respect to the pyridine N–C bond. This enables the NH group to act as a hydrogen-bond donor to one apical formate. The resulting complex has a coordination number of four (CN = 4). In the second, denoted as *cis*, the C=O bond being *cis* to the pyridine N–C bond, the oxygen binds to  $\text{Cu}^{2+}$ , the coordination of which becomes six (CN = 6). This last arrangement is the one observed in the parent **C1** and **C2** crystal structures.<sup>6</sup>

Table 5 reports the in vacuo energy balances for complexation of **C1a** and **C2a**. The reported energy values represent the differences between the actual values in the complex and twice the corresponding values in the isolated flexible ligand in its energy-minimized conformation. From the tabulated values, we can see that HF, DFT, and SIBFA computations indicate complex **C1a** to be more stable than complex **C2a**. Both HF and DFT, furthermore, indicate complexation to occur more favorably in the *trans* mode than in the *cis* mode.



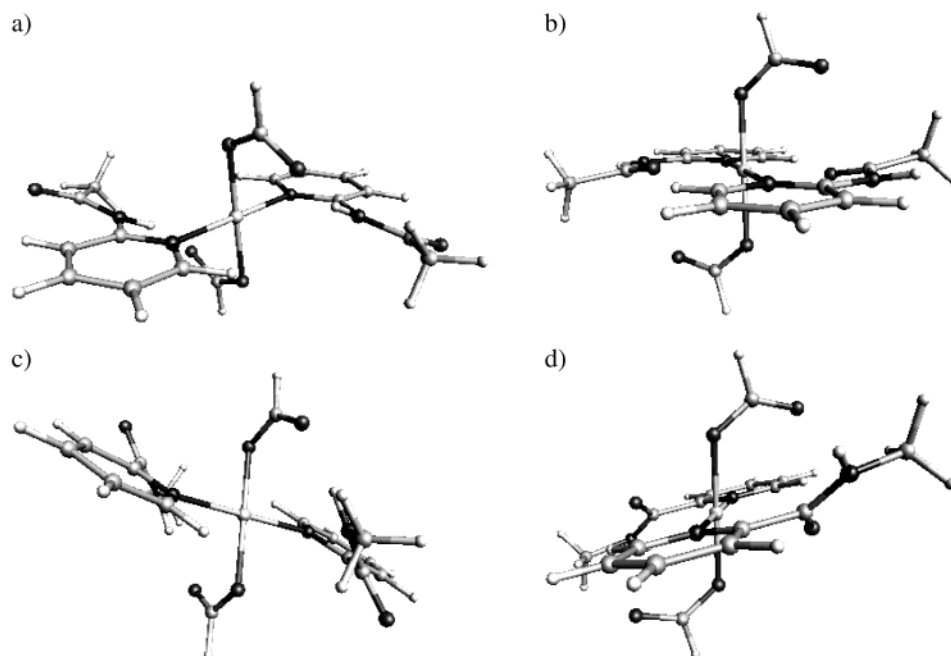


**Figure 5.** Optimized arrangements of the **C1a** (a and b) and **C2a** (c and d) complexes in the trans and cis arrangements.

For all four complexes,  $\Delta E(\text{SIBFA})$  without dispersion reproduces  $\Delta E(\text{HF})$  with a relative error inferior to 2%. However, the trans versus cis preference is, in the case of **C1a**, much smaller than the one predicted from the HF computations. It is of 8 out of 630 kcal/mol prior to inclusion of the 2-fold torsional barrier and reduces to 3 kcal/mol after inclusion of the latter, whereas  $\Delta E(\text{HF})$  gives a difference of 16 kcal/mol. The reduction of the  $\Delta E(\text{SIBFA})$  difference when the torsional barrier is included is due to the lesser deviation from coplanarity of the pyridine and amide ligands in the cis than in the trans complexes. Inclusion of  $E_{\text{disp}}$  favors the **C1a**, cis complex, resulting into a more favorable  $\Delta E_{\text{tot}}(\text{SIBFA})$  value for the cis than for the trans mode. Such a preference is opposite to the DFT results, even though the numerical values of  $\Delta E_{\text{tot}}(\text{SIBFA})$  match the DFT ones to within 5% relative error. This may indicate the limitations inherent in the formulation of  $E_{\text{disp}}$  and the possible need to further account for its nonadditive character in polyligated metal complexes, as outlined earlier<sup>17,20,21</sup>. The energy gain upon passing from uncorrelated HF to correlated DFT calculations is smaller in the cis complex than in the trans one (−54.7 versus −65.8 kcal/mol, respectively) whereas the opposite trend is found with  $E_{\text{disp}}$ .

For **C2a**, the SIBFA computations give the trans mode to be more favorable energetically than the cis mode, both with and without the dispersion energy term. The HF and DFT energy values are reproduced with relative errors of 2% and 4%, respectively. It is also noteworthy that for all four considered complexes the values of  $\Delta E(\text{DFT})$  at the SIBFA-minimized conformations are close to those resulting from DFT-energy-minimization.

The QC values reported in this study serving as benchmarks for the development of  $\text{Cu}^{2+}$  potentials in polarizable molecular mechanics have highlighted the quality but also the shortcomings of the present formulation of SIBFA for this cation. Thus, the values of  $\Delta E_{\text{tot}}$  could reproduce those from corresponding single-point QC computations with relative errors <5%. Such an accuracy enabled us to account for the more favorable complexation energies of **C1a** than **C2a** and for that of the trans isomer of **C2a** than the cis isomer. However, the SIBFA computations also led to a corresponding preferential stability

of **C1a** cis than **C1a** trans, whereas the QC computations gave the reverse. Refining the SIBFA potential could take place along the three following lines: (a) explicit inclusion of ligand-field effects<sup>10,11</sup> (Piquemal et al., work in progress); (b) improvement of the SIBFA electrostatic term (Piquemal et al., work in progress);<sup>41</sup> and (c) inclusion into  $E_{\text{rep}}$  of a “three-body” term involving Cu(II) and the combination of all the pairs of its ligands. Such a term has been explicitly included in studies of metal ion solvation<sup>48,49</sup> to account for the nonadditivity of the exchange component which originates from the reorthogonalization of the wave functions of the monomers. Its inclusion, in light of the results of  $E_1$  nonadditivity reported in ref 17, should reduce the  $E_1$  energy difference that occurs in favor of complexes with a larger coordination number, as exemplified in the cis complexes of **C1a** and **C2a** (CN = 6) versus the trans ones (CN = 4).

**5. Structural Analyses of C1 and C2.** Energy-minimizations using SIBFA bore on the six intermolecular variables defining the position of approach of each interacting partner in the complexes **C1** and **C2** (three variables for  $\text{Cu}^{2+}$ ) together with the torsional angles along the junctional bonds of the flexible ligands. They were performed in water using the continuum reaction field procedure.

The energy-minimized geometries were compared to the crystallographic structures. Superimposition on heavy atoms of X-ray diffraction (XRD) and SIBFA structures yields a RMS less than 0.3 Å (Figure 6).

The crystal structures are thus reproduced with acceptable accuracy and show a good agreement on distances, angles, and dihedrals (Table 6). In fact, the distances and the valence angles between the ligands and the  $\text{Cu}^{2+}$  ion are evaluated with a maximal deviation of 0.16 Å and 3.86° respectively. However, the distances between  $\text{Cu}^{2+}$  and the molecules of methanol or perchlorate located in apical position are underestimated because the SIBFA procedure does not yet account for the Jahn–Teller distortion observed for  $\text{Cu}^{2+}$  complexes. The largest deviations affecting the dihedrals are observed for the methoxyphenyl groups of both ligands (up to 34.0°). However, the values obtained with the SIBFA method are consistent with a statistical

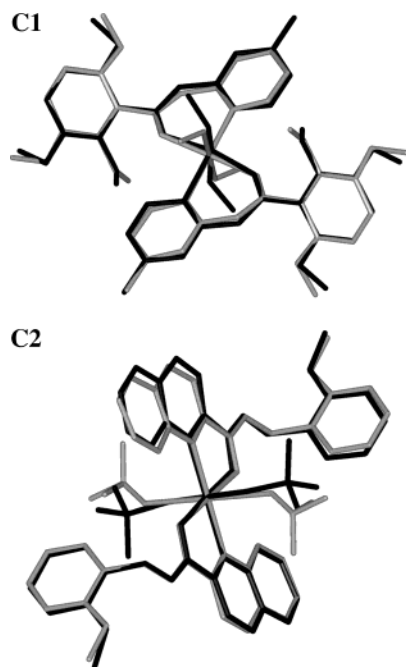


**Figure 6.** Superimposition of XRD (gray) and SIBFA (black) structures of complexes **C1** and **C2**. A RMS <0.3 Å has been obtained on heavy atoms.

analysis performed on related fragments in the Cambridge structural database (CSD).<sup>50</sup>

**6. Energetics: Stability Analysis of C1 and C2.** We have previously shown that under the biological testing conditions, that is, in the presence of acetate anions (aqueous assay buffer: NaOAc 0.1M, pH=5.5), **C1** still exists as a complex, whereas **C2** releases its ligands in favor of acetate.<sup>7</sup> Using the SIBFA methodology, we analyzed the relative stabilities of **C1** and **C2** when acetate anions are competing.

The Cu<sup>2+</sup> acetate complexation has been previously reported. In the solid state, the Cu<sup>2+</sup> acetate monohydrate is observed as a dimer with the general formula [Cu(OAc)<sub>2</sub>(H<sub>2</sub>O)]<sub>2</sub>: the two Cu<sup>2+</sup> are bridged symmetrically by the four acetate ligands, with the two copper ions antiferromagnetically coupled.<sup>51</sup> In solution, a dissociation mechanism occurs leading to the mononuclear form of the complex.<sup>52</sup> The stability constants of this mononuclear complex are quite low ( $K_1 = [\text{ML}]/[\text{M}][\text{L}] = 0.490 \times 10^2$ ;  $K_2 = [\text{ML}_2]/[\text{ML}][\text{L}] = 0.107 \times 10^2$ ;  $\beta_2 = [\text{ML}_2]/[\text{M}][\text{L}]^2 = 5.25 \times 10^2$ ).<sup>53</sup> Therefore, at pH 5.5, the main species observed is the free cupric ion (about 90%), whereas [CuOAc]<sup>+</sup> represents only about 10% (we can also note that there are only traces of Cu(OAc)<sub>2</sub> at this pH). [The species distribution in functions of pH have been evaluated with the aid of the SPECIES.EXE subprogram included in the SC-Database (Pettit, L. D.; Powell, K. J. *Stability Constants Database (SC-Database)*; IUPAC and Academic Software: Yorks, U.K., 1999).] We compared the SIBFA stabilization energy of **C1** and **C2** with waters (W) in apical positions to that of Cu<sup>2+</sup> acetate complexes ([CuOAc(H<sub>2</sub>O)<sub>5</sub>]<sup>+</sup> and Cu(OAc)<sub>2</sub>(H<sub>2</sub>O)<sub>4</sub>), after energy optimization in water using the equations:  $\Delta E_{\text{stab}} = E_{\text{C}} + E_{\text{solvC}} - 2(E_{\text{L}} + E_{\text{solvL}}) - 2E_{\text{solvW}} - E_{\text{solvCu}}$  for **C1** and **C2**, and  $\Delta E_{\text{stab}} = E_{\text{C}} + E_{\text{solvC}} - x(E_{\text{OAc}} + E_{\text{solvOAc}}) - yE_{\text{solvW}} - E_{\text{solvCu}}$  for Cu<sup>2+</sup> acetate (with  $x$  = number of acetate ion in the complex and  $y$  = number of water molecule in the complex). The results of these calculations are reported in Table 7. In Tables 7 and 8, the significance of the energy values is the same as in Table 5.

The  $\Delta E_{\text{stab}}$  of **C1** and **C2** are very different, with **C1** being more stable by 25 kcal/mol. This large energy difference could

be overestimated because of the simplified model and absence of counterions.

Two types of complexation were considered for Cu(OAc)<sub>2</sub>(H<sub>2</sub>O)<sub>4</sub>. In the first, Cu<sup>2+</sup> binds directly and monodentately to one acetate ion and to all four water molecules, leading to a coordination number of five (Cu(OAc)<sub>2</sub>(H<sub>2</sub>O)<sub>4</sub>, CN = 5). The second acetate anion is bound to copper through two water molecules. After SIBFA minimization, we obtained a structure in which all water ligands are hydrogen bonded to one acetate ion, the indirectly bound acetate receiving a proton from three waters. In the second, Cu<sup>2+</sup> binds directly and monodentately to each acetate and to the four waters leading to a coordination number of six (Cu(OAc)<sub>2</sub>(H<sub>2</sub>O)<sub>4</sub>, CN = 6). Each in-plane water is hydrogen bonded with one acetate anion. The two types of complexation for Cu(OAc)<sub>2</sub>(H<sub>2</sub>O)<sub>4</sub> give similar stabilities with only 0.5 kcal/mol in favor of the pentacoordinated complex (Cu(OAc)<sub>2</sub>(H<sub>2</sub>O)<sub>4</sub>, CN = 5), whereas [CuOAc(H<sub>2</sub>O)<sub>5</sub>]<sup>+</sup> is less stable than the two Cu(OAc)<sub>2</sub>(H<sub>2</sub>O)<sub>4</sub> arrangements. The comparison of the stabilization energies of **C1** and **C2** with that of the copper acetate complexes is interesting because it can highlight the observed acetate mediated dissociation mechanism occurring with these complexes. In fact, **C2** has a low stabilization energy: it is less stable than both Cu<sup>2+</sup> acetate complexes Cu(OAc)<sub>2</sub>(H<sub>2</sub>O)<sub>4</sub> ( $\Delta E_{\text{stab}} = 4.6$  and 5.1 kcal/mol respectively). Unlike **C2**, **C1** has a larger stability than the Cu<sup>2+</sup> acetate complexes in the aqueous medium. In this case, the stability gains are over 20 kcal/mol. These theoretical results are qualitatively consistent with the experiment which shows a partial release of Cu<sup>2+</sup> in the assay buffer from complex **C1** and a total release of Cu<sup>2+</sup> from complex **C2**.

**7. Ligand Structure Influence on Stability.** We have investigated the influence of the methoxyphenyl substituents on stability. We calculated the stabilization energy ( $\Delta E_{\text{stab}}$ ) in water of optimized **C1** derivatives in which the ortho and/or meta methoxy groups have been systematically removed, i.e., the complexes **C1b** to **C1g** formed from the following ligands: *N*1-(4-methyl-2-pyridyl)-benzamide (**L1b**), *N*1-(4-methyl-2-pyridyl)-3-methoxybenzamide (**L1c**), *N*1-(4-methyl-2-pyridyl)-3,6-dimethoxybenzamide (**L1d**), *N*1-(4-methyl-2-pyridyl)-2,3-dimethoxybenzamide (**L1e**), *N*1-(4-methyl-2-pyridyl)-2-methoxybenzamide (**L1f**), and *N*1-(4-methyl-2-pyridyl)-2,6-dimethoxybenzamide (**L1g**). All of these complexes were built with water molecules in apical positions. The results of these calculations and the comparison of the different  $\Delta E_{\text{stab}}$  values are summarized in Table 8 and illustrated in Figure 7.

The results show that the stabilization of **C1** is mainly induced by the ortho methoxyphenyl substituents, whereas the meta methoxy group has a weaker influence on the complex stability or is even rather unfavorable. In fact, when we compare the  $\Delta E_{\text{stab}}$  of **C1**, **C1c**, **C1d**, and **C1e**, we can see that each ortho methoxy group contributes to **C1** stabilization by about 6 kcal/mol. The meta methoxy removal in **C1g** induces a 2 kcal/mol destabilization of the complex. Addition of one ortho methoxy group to the benzamide derivative **C1b** stabilizes the resulting complex **C1f** by about 6 kcal/mol. When a second ortho methoxy substituent is added (**C1g**), a supplementary 3 kcal/mol stabilization energy is observed. On the other hand, addition of a meta methoxy substituent in **C1c** induces a 2 kcal/mol destabilization compared to **C1b**. These results mainly arise from the antagonist behavior of the electrostatic and repulsive components of the SIBFA interaction energy. In fact, the repulsive component  $E_{\text{rep}}$  is affected by the presence of the three methoxy substituents (Table 8). The benzamide derivative **C1b**, which does not contain any methoxy groups is the most

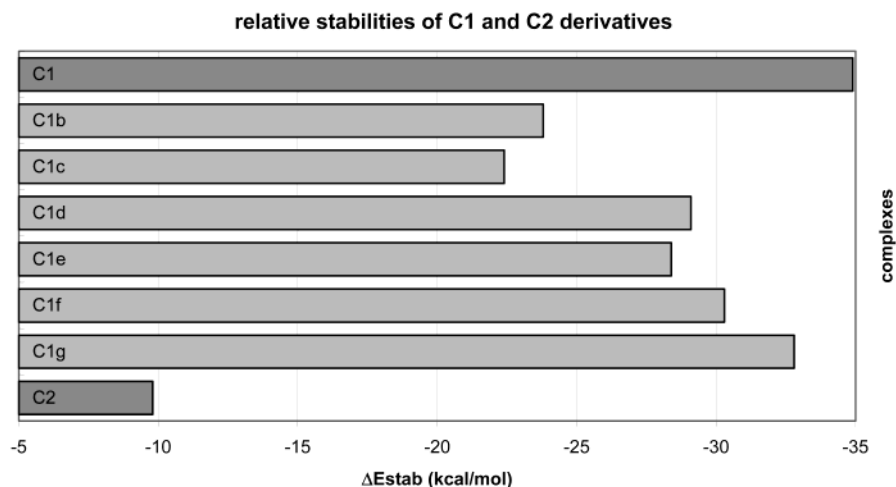


**Figure 7.** Relative stabilities of **C1** and **C2** derivatives.

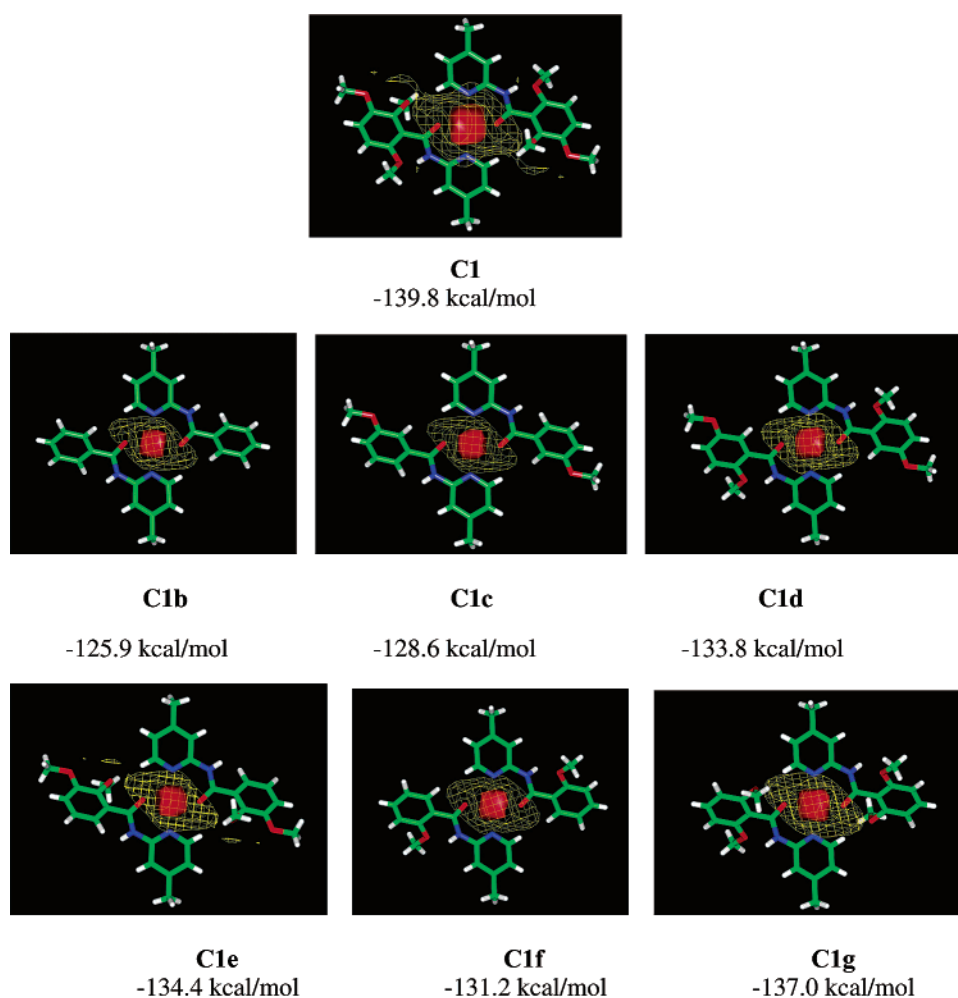


**Figure 8.** InsightII<sup>55</sup> visualization of the MEP calculated (HF/6-31G\*) for the crystal structures of **C1** and its derivatives without the  $\text{Cu}^{2+}$  ion. The isocontours are represented at  $-100$  kcal/mol (red) and  $-50$  kcal/mol (yellow), and the color code is green for carbon, white for hydrogen, blue for nitrogen, and red for oxygen atoms. The minimum potential energies obtained at the cupric ion position are mentioned.

favorable from a repulsive point of view and the addition of a meta methoxy (**C1c**) or an ortho methoxy (**C1f**) results in an increase of  $E_{\text{rep}}$  of about 3 and 10 kcal/mol, respectively. On the other hand, we can see from the  $E_{\text{MTP}}$  in Table 8 that the three methoxy substituents induce an electrostatic stabilization of the **C1** complex. This stabilization is mainly due to the ortho methoxy groups, but interestingly, the  $E_{\text{MTP}}$  is by 20 kcal/mol lower for the 2,3-dimethoxybenzamide derivative (**C1e**) than for the 3,6-dimethoxybenzamide (**C1d**).

It was interesting to compare these SIBFA  $E_{\text{MTP}}$  with the ab initio molecular electrostatic potentials (MEP, HF/6-31G\*) at  $\text{Cu}^{2+}$  in the **C1** derivatives. The MEP were calculated for **C1** to **C1g** constructed from the **C1** crystal structure without the cupric ion and the apical molecules. The minimum potential energies obtained at the cupric ion position are presented in Figure 8.

To compare these ab initio MEP calculations with the SIBFA results, we reevaluated the SIBFA electrostatic contribution on

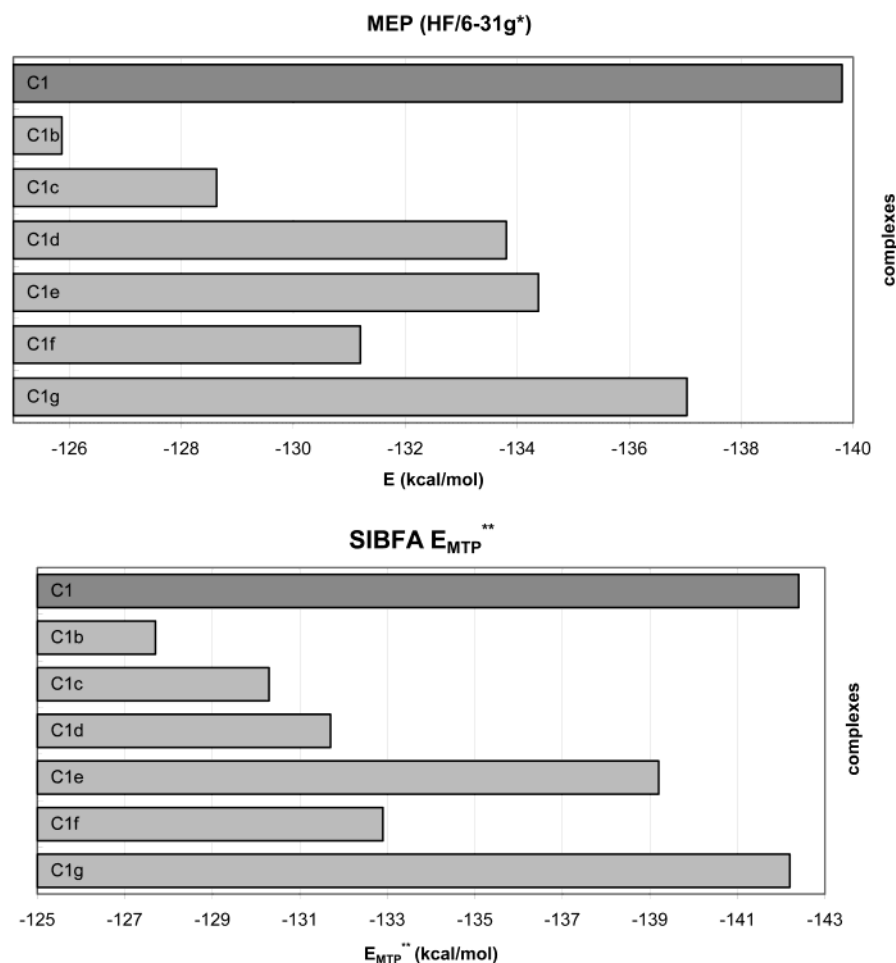


**Figure 9.** Comparison of the minimum potential energies obtained at the cupric ion position of the **C1** derivatives and the corresponding SIBFA  $E_{MTP}^{**}$  values.

the **C1** derivatives without apical water molecules and with a net charge of +1 on the copper ion. The resulting  $E_{MTP}^{**}$  are reported in Table 8. We can see from Figure 9 that there is a good correlation between the SIBFA  $E_{MTP}^{**}$  and the ab initio electrostatic potential encountered at the copper position. The MEP results show as well that the three methoxy substituents contribute to reinforce the attractive well located at the cupric ion position. This effect can be mainly attributed to the ortho methoxy groups (contribution of one ortho methoxy group: about 6 kcal/mol; contribution of the meta methoxy group: about 3 kcal/mol), which is consistent with the SIBFA results.

### Conclusions and Perspectives

We previously developed a novel family of  $\text{Cu}^{2+}$  complexes which act as HIV-1 protease inhibitors. We have focused our attention on complexes formed from the binding of two bidentate ligands (e.g., nitrogen-containing heterocycles connected to a carboxamide moiety and an appending aromatic ring) to a central  $\text{Cu}^{2+}$  cation.<sup>6</sup> These molecules were designed to interact with the active site of the protease and inhibit its proteolytic activity. We have previously shown that some of these complexes were inactive at inhibiting HIV-1 PR because of their poor stability in solution.<sup>7</sup> In this work, we investigated the molecular characteristics responsible for the stability of such complexes, as exemplified by **C1** and **C2**, made out from dimers of a *N*-amido-linked pyridine and a *C*-amido-linked quinoline, respectively.

In a first step, we have extended the calibration of the SIBFA polarizable molecular mechanics procedure to the open-shell

$\text{Cu}^{2+}$  cation. This was done by performing energy-decomposition analyses and correlated MP2 calculations of its monoligated binding energies to a series of N-, O-, and S-containing ligands. The accuracy of the procedure was tested by several comparisons with HF, DFT, and MP2 calculations of the binding energies in polycoordinated complexes of one or two  $\text{Cu}^{2+}$  cations. In such arrangements, and in the absence of the dispersion energy component,  $\Delta E(\text{SIBFA})$  reproduced  $\Delta E(\text{HF})$  with a relative error <3%. At the correlated level, the agreement between the values of  $\Delta E_{\text{tot}}(\text{SIBFA})$  including the  $E_{\text{disp}}$  component and correlated quantum-chemical values remained satisfactory, the SIBFA interaction energies being closer to the MP2 than to the DFT ones.

In a second step, we have used the SIBFA procedure to study the structural and energetical features of the **C1** and **C2** complexes. The energy balances taking into account the effects of solvation have highlighted the greater stability of **C1** than **C2** against dissociation by acetate, in agreement with experimental results. This study has also pointed out the ortho methoxyphenyl substituents as crucial components for the higher stability of **C1**. In fact, these calculations have quantified the stabilizing role of the ortho-methoxy substituents on the phenyl rings of **C1** by evaluating the effect of removal of one up to three ortho-methoxy groups on the total binding energies. Moreover, we have found a correlation between the values of the electrostatic component of the interaction energy,  $E_{MTP}$ , and those of the ab initio molecular electrostatic potential (MEP) at the  $\text{Cu}^{2+}$  position. In the future, the docking of **C1** and analogues into the active site of the HIV-1 protease will be undertaken. It



will be instructive in this respect to delineate the role of ring substituents and added aromatic/apolar appendages to the molecule and how they could contribute separately, on one hand, to the intrinsic stability of such Cu<sup>2+</sup> organometallic complexes, and, on the other hand, to their actual interactions with protease residues at the active site.

**Acknowledgment.** The ab initio (DFT and MP2) computations were performed on the computers of IDRIS, Orsay, France. Several computations using the SIBFA procedure were performed at CINES, Montpellier, France. M.L. and F.L. thank the FRIA and the FNRS for financial support and the Facultés Universitaires Notre-Dame de la Paix for use of computing facilities.

**Supporting Information Available:** Parameters used in the calibration of Cu<sup>2+</sup>. This material is available free of charge via the Internet at <http://pubs.acs.org>.

## References and Notes

- (1) Sadler, P. J. *Inorganic chemistry and drug design. Advances in inorganic chemistry*; Academic Press: New York, 1991.
- (2) Louie, A. Y.; Meade, T. J. *Chem. Rev.* **1999**, 99, 2711.
- (3) Lippard, S. J. In *Bioinorganic chemistry*; Bertini, I., et al., Eds.; University Science: Mill Valley, CA, 1994.
- (4) Katz, B. A.; Clark, J. M.; Finer-Moore, J. S.; Jenkins, T. E.; Johnson, C. R.; Ross, M. J.; Luong, C.; Moore, W. R.; and Stroud, R. M. *Nature* **1998**, 391, 608. Janc, J. W.; Clark, J. M.; Warne, R. L.; Elrod, K. C.; Katz, B. A.; and Moore, W. R. *Biochemistry* **2000**, 39, 4792. Berners-Price, S. J.; Sadler, P. J. *Coord. Chem. Rev.* **1996**, 151, 1.
- (5) Lebon, F.; de Rosny, E.; Reboud-Ravaux, M.; Durant, F. *Eur. J. Med. Chem.* **1998**, 33, 733. Lebon, F.; Ledecq, M.; Dieu, M.; Demazy, C.; Remacle, J.; Lapouyade, R.; Kahn, O.; Durant, F. *J. Inorg. Biochem.* **2001**, 86, 547.
- (6) Lebon, F.; Ledecq, M.; Benatallah, Z.; Sicsic, S.; Lapouyade, R.; Kahn, O.; Garçon, A.; Reboud-Ravaux, M.; and Durant, F. *J. Chem. Soc., Perkin Trans. 2* **1999**, 4, 795.
- (7) Lebon, F.; Boggetto, N.; Ledecq, M.; Durant, F.; Benatallah, Z.; Sicsic, S.; Lapouyade, R.; Kahn, O.; Mouithys-Mickalad, A.; Deby-Dupont, G.; Reboud-Ravaux, M. *Biochem. Pharmacol.* **2002**, 63, 1863.
- (8) Flexner, C. *New Engl. J. Med.* **1998**, 338, 1281. Molla, A.; Granneman, G. R.; Sun, E.; Kempf, D. J. *Antiviral. Res.* **1998**, 39, 1. Brik, A.; Wong, C.-H. *Org. Biomol. Chem.* **2003**, 1, 5.
- (9) Comba, P.; Sickmüller, A. F. *Inorg. Chem.* **1997**, 36, 4500. Bernhardt, P. V.; Comba, P. *Inorg. Chem.* **1992**, 31, 2638. Sabolović, J.; Tauterman, C. S.; Loerting, T.; Liedl, K. R. *Inorg. Chem.* **2003**, 42, 2268. Kaitner, B.; Maulić, N.; Pavlović, G.; Sabolović, J. *Polyhedron* **1999**, 18, 2301.
- (10) Deeth, R. J.; Paget, V. J. *Chem. Soc., Dalton Trans.* **1997**, 537. Burton, V. J.; Deeth, R. J.; Kemp, C. M.; Gilbert, P. J. *J. Am. Chem. Soc.* **1995**, 117, 8407.
- (11) Gerloch, M.; Harding, J. H.; Woolley, R. G. *Struct. Bonding* **1981**, 46, 1. Woodley, S. M.; Battle, P. D.; Catlow, C. R. A.; Gale, J. D. *J. Phys. Chem. B* **2001**, 105, 6824.
- (12) Gresh, N.; Claverie, P.; Pullman, A. *Theor. Chim. Acta* **1984**, 66, 1.
- (13) Gresh, N.; Claverie, P.; Pullman, A. *Theor. Chim. Acta* **1985**, 67, 11. Gresh, N.; Leboeuf, M.; Salahub, D. R. In *Modelling the hydrogen bond*; Smith, D. A., Ed.; American Chemical Society Symposia; American Chemical Society: Washington, DC, 1994.
- (14) Gresh, N.; Claverie, P.; Pullman, A. *Int. J. Quantum Chem.* **1986**, 29, 101.
- (15) Stevens, W. J.; Fink, W. *Chem. Phys. Lett.* **1987**, 139, 15.
- (16) Gresh, N. *J. Comput. Chem.* **1995**, 16, 856.
- (17) Tiraboschi, G.; Roques, B.-P.; Gresh, N. *J. Comput. Chem.* **1999**, 20, 1379.
- (18) Gresh, N.; Sponer, J. *J. Phys. Chem. B* **1999**, 103, 11415.
- (19) Rogalewicz, F.; Ohanessian, G.; Gresh, N. *J. Comput. Chem.* **2000**, 21, 963.
- (20) Tiraboschi, G.; Gresh, N.; Giessner-Prettre, C.; Pedersen, L. G.; Deerfield, D. W. *J. Comput. Chem.* **2000**, 21, 1011.
- (21) Tiraboschi, G.; Fournié-Zaluski, M.-C.; Roques, B.-P.; Gresh, N. *J. Comput. Chem.* **2001**, 22, 1038.
- (22) Gresh, N.; Policar, C.; Giessner-Prettre, C. *J. Phys. Chem. A* **2002**, 106, 5660.
- (23) Gresh, N.; Garmer, D. R. *J. Comput. Chem.* **1996**, 17, 1481. Garmer, D. R.; Gresh, N. *J. Am. Chem. Soc.* **1994**, 116, 6.
- (24) Gresh, N.; Roques, B.-P. *Biopolymers* **1997**, 41, 145. Garmer, D. R.; Gresh, N.; Roques, B. P. *Proteins* **1998**, 31, 42.
- (25) Antony, J.; Gresh, N.; Olsen, L.; Hemmingsen, L.; Schofield, C. J.; Bauer, R. *J. Comput. Chem.* **2002**, 23, 1281.
- (26) Vigné-Maeder, F.; Claverie, P. *J. Chem. Phys.* **1988**, 88, 4934.
- (27) Gresh, N. *J. Phys. Chem. A* **1998**, 101, 8680. Gresh, N.; Guo, H.; Salahub, D. R.; Roques, B. P.; Kafafi, S. A. *J. Am. Chem. Soc.* **1999**, 121, 7885.
- (28) Garmer, D. R.; Stevens, W. J. *J. Phys. Chem.* **1989**, 93, 8263.
- (29) Schmidt, M. W.; Baldrige, K. K.; Boatz, J. A.; Elbert, S. T.; Gordon, M. S.; Jensen, J. H.; Koseki, S.; Matsunaga, N.; Nguyen, K. A.; Su, S.; Windus, T. L.; Dupuis, M.; Montgomery, J. A., Jr. *J. Comput. Chem.* **1993**, 14, 1347.
- (30) Creuzet, S.; Langlet, J.; Gresh, N. *J. Chim. Phys., PCB* **1991**, 88, 2399.
- (31) Godbout, N.; Salahub, D. R.; Andzelm, J.; Wimmer, E. *Can. J. Chem.* **1992**, 70, 560.
- (32) Stevens, W. J.; Basch, H.; Krauss, M. *J. Chem. Phys.* **1984**, 81, 6026.
- (33) Ren, P.; Ponder, J. W. *J. Comput. Chem.* **2002**, 23, 1497.
- (34) Gresh, N.; Derreumaux, P. *J. Phys. Chem. B* **2003**, 104, 4862.
- (35) Evangelakis, G.; Rizos, J.; Lagaris, I.; Demetropoulos, G. N. *Comput. Phys. Commun.* **1987**, 46, 401.
- (36) Langlet, J.; Claverie, P.; Caillet, J.; Pullman, A. *J. Phys. Chem.* **1988**, 92, 1617.
- (37) Langlet, J.; Gresh, N.; Giessner-Prettre, C. *Biopolymers* **1995**, 36, 765.
- (38) Bagus, P. S.; Illas, F. *J. Chem. Phys.* **1992**, 96, 8962.
- (39) Dupuis, M.; Marquez, A.; Davidson, E. R. *Hondo 95.3, Quantum Chemistry Program Exchange (QCPE)*; Indiana University: Bloomington, IN.
- (40) Marquez, A. *CSOV implementation*, unpublished work.
- (41) Gordon, M. S.; Freitag, M. A.; Bandyopadhyay, P.; Jensen, J. H.; Kairys, V. *J. Phys. Chem. A* **2001**, 105, 293.
- (42) Corongiu, G.; Clementi, E. *J. Chem. Phys.* **1978**, 69, 4885.
- (43) El-Nahas, A. M.; Tajima, N.; Hirao, K. *Chem. Phys. Lett.* **2000**, 318, 333.
- (44) Stace, A. J.; Walker, N. R.; Wright, R. R.; Firth, S. *Chem. Phys. Lett.* **2000**, 329, 173.
- (45) Concha, N. O.; Rasmussen, B. A.; Bush, K.; Herzberg, O. *Structure* **1996**, 4, 823. Demoulin, D.; Pullman, A.; Sarkar, B. *J. Am. Chem. Soc.* **1977**, 99, 8498. Monard, G.; Merz, K. M., Jr. *Acc. Chem. Res.* **1999**, 32, 904.
- (46) Olsson, M. H.; Ryde, U. *J. Am. Chem. Soc.* **2001**, 123, 7866.
- (47) Wilcox, E. A. *Chem. Rev.* **1996**, 96, 2435.
- (48) Lybrand, T. P.; Kollman, P. A. *J. Chem. Phys.* **1985**, 83, 2923.
- (49) Dubois, V.; Archirel, P.; Boutin, A. *J. Phys. Chem. B* **2001**, 105, 9363.
- (50) Allen, F. H.; Kennard, O. *Chem. Des. Autom. News* **1993**, 8, 1 & 31.
- (51) Harcourt, R. D.; Skrezenek, F. L.; MacLagan, R. G. A. R. *J. Am. Chem. Soc.* **1986**, 108, 5403.
- (52) Tackett, J. E. *Appl. Spectrosc.* **1989**, 43, 483. Sharrock, P.; Melnik, M. *Can. J. Chem.* **1985**, 63, 52. Szpakowska, M.; Uruska, I. *Pol. J. Chem.* **1980**, 54, 1661. Zielkiewicz, J.; Uruska, I.; Szpakowska, M. *Pol. J. Chem.* **1991**, 65, 177.
- (53) Vetere, V. F.; Romagnoli, R. *Analyst* **1991**, 116, 937.
- (54) Bone, R.; Vacca, J. P.; Anderson, P. S.; Holloway, M. K. *J. Am. Chem. Soc.* **1991**, 113, 9382.
- (55) InsightII; Accelerlys: San Diego, CA, 2000.